J Neuropathol Exp Neurol
Vol. 65, No. 2
February 2006
pp. 162–175


ORIGINAL ARTICLE

# Neuregulin Growth Factors and Their ErbB Receptors Form a Potential Signaling Network for Schwannoma Tumorigenesis

Mark S. Stonecypher, BS, Abhik Ray Chaudhury, MBBS, Stephanie J. Byer, BS, and Steven L. Carroll, MD, PhD

**Abstract**

Sporadic and neurofibromatosis type 2-associated schwannomas contain a glial growth factor (GGF)-like activity that has been hypothesized to promote neoplastic Schwann cell mitogenesis. It is not known whether this GGF-like activity is neuregulin-1 (NRG-1), an epidermal growth factor (EGF)-related molecule that regulates the proliferation, survival, and differentiation of developing Schwann cells, the related factor NRG-2, or another NRG/EGF ligand. We report that neoplastic Schwann cells within schwannomas overexpress multiple α and β transmembrane precursors from the class II and class III NRG-1 subfamilies. NRG-2 α and β transcripts are similarly overexpressed in some tumors. Of the other 8 known NRG/EGF ligands, only heparin-binding EGF, epiregulin, and TGFα are detectable in schwannomas. Neoplastic Schwann cells almost uniformly express erbB2 and erbB3, 2 membrane receptor tyrosine kinases mediating NRG-1 and NRG-2 action. Expression of the NRG receptor erbB4 and EGF receptor is also evident in schwannomas, but is more limited, occurring in only a subset of these tumors. ErbB2, the preferred dimerization partner for all erbB kinases, is constitutively phosphorylated in schwannomas. These observations suggest that autocrine, paracrine, and/or juxtacrine NRG-1/NRG-2 signaling promotes schwannoma pathogenesis and that this signaling pathway may be an important therapeutic target in schwannomas.

**Key Words:** Epidermal growth factor, erbB receptors, Neuregulin, Neurofibromatosis, Schwannoma.

## INTRODUCTION

Schwannomas, the third most common type of primary nervous system neoplasm, are derived from Schwann cells, the myelinating glia of peripheral nerves. These benign peripheral nerve sheath tumors arise most frequently from sensory nerves, with common sites of occurrence including nerves in the head and neck region, cranial and spinal nerve roots, and nerves along the extensor surfaces of the extremities (1). Schwannomas typically occur as single lesions in otherwise normal patients. However, individuals with the autosomal-dominant tumor susceptibility syndrome neurofibromatosis type 2 (NF2) characteristically develop bilateral vestibular nerve (acoustic) schwannomas and multiple schwannomas of spinal dorsal nerve roots (2, 3). Multiple subcutaneous and spinal root schwannomas are also a feature of schwannomatosis, a rare genetic disorder distinct from NF2 (4). Sporadic, NF2-, and schwannomatosis-associated schwannomas frequently occur in confined spaces within the cranium and spinal column, where their impingement on nerves and the central neuraxis results in considerable patient morbidity. Surgical resection is the standard approach to treating these tumors but can be rendered difficult by tumor size, multiplicity, or location. The alternative is radiotherapy or radiosurgery, both of which have shown limited success, particularly when treating larger neoplasms (5). Given these limitations, there is considerable interest in defining the molecular abnormalities promoting schwannoma tumorigenesis and using this information to develop new, more effective treatments for these tumors.

The genetic alterations involved in schwannoma pathogenesis are poorly understood. It is known that patients with NF2 carry a germline mutation in the NF2 tumor-suppressor gene on chromosome 22q12 and, in keeping with the proposed function of this gene, develop schwannomas when the remaining functional copy of the NF2 gene is lost (6, 7). Both sporadic and NF2-associated schwannomas demonstrate a near-universal loss of expression of merlin (8–10), the product of the NF2 locus. Merlin (also known as schwannomin) is related to the ERM (ezrin, radixin, and moesin) proteins and has been found to modulate cell motility and to suppress mitogenesis (3). Based on these actions, it is thought that a loss of merlin expression in Schwann cells leads to inappropriate Schwann cell growth and the formation of schwannomas. Other genetic abnormalities such as chromosome 1p loss (11) and 9q34 gain (12) have also been identified in small subsets of schwannomas, but the essential genes within these regions remain to be defined.

Overexpression of growth factors and/or their receptors may also contribute to the pathogenesis of sporadic and NF2-associated schwannomas. In 1986, Brockes et al reported that

From the Departments of Cell Biology (MSS, SLC) and Pathology (SJB, SLC), The University of Alabama at Birmingham, Birmingham, Alabama; and the Department of Pathology (ARC), Ohio State University, Columbus, Ohio.

Send correspondence and reprint requests to: Dr. Steven L. Carroll, Division of Neuropathology, Department of Pathology, The University of Alabama at Birmingham, 1720 Seventh Avenue South, SC843, Birmingham, AL 35294-0017; E-mail: carroll@path.uab.edu

This study was supported by National Institute of Neurological Diseases and Stroke grant R01 NS048353.

extracts from 3 NF2-associated vestibular schwannomas and 5 of 7 sporadic vestibular schwannomas contained a Schwann cell growth-promoting activity similar to that present in partially purified preparations of bovine pituitary glial growth factor (GGF) (13). Pituitary GGF was subsequently purified and cloned, leading to the finding that pituitary-derived GGF proteins were members of the neuregulin-1 (NRG-1) family of growth factors, a group of epidermal growth factor (EGF)-related molecules that act through erbB membrane tyrosine kinases to stimulate the proliferation, survival, and migration of Schwann cells during development (14–16). The GGF-like activity present in schwannomas, however, has never been definitively identified. Although it is tempting to assume that this activity similarly represents NRG-1 proteins, other NRG-related molecules, including NRG-2, NRG-3, and NRG-4, have recently been identified. Some of these molecules have biochemical and functional characteristics similar to NRG-1, raising the question of whether the GGF-like activity in schwannomas instead corresponds to one of these other growth factors. As an initial step toward defining the GGF-like activity present in schwannomas, we have systematically analyzed the expression of specific isoforms of NRG-1 and NRG-2 and of all the other known NRG and EGF family growth factors in human schwannomas. Because each erbB kinase differs in its affinity for these ligands, we have also examined the expression of all 4 erbB receptors in schwannomas and ascertained whether there is evidence of constitutive erbB activation in these tumors.

## MATERIALS AND METHODS

### Study Cases

Experiments described in this article were approved by the Institutional Review Boards for Human Use of the University of Alabama at Birmingham and Washington University School of Medicine. Paraffin blocks of human schwannoma cases were obtained from the files of the Departments of Pathology of Washington University School of Medicine (St. Louis, MO) and the University of Alabama School of Medicine (Birmingham, AL). Frozen, surgically resected schwannoma tissue was provided by the Southern Division of the Cooperative Human Tissue Network/University of Alabama at Birmingham Tumor Bank and the University of Alabama Brain Tumor Bank.

### Antisera and Immunohistochemical Reagents

We have previously described the production and characterization of a rabbit polyclonal antibody that recognizes the EGF-like common domain found in all biologically active NRG-1 isoforms (a "pan NRG-1" antibody) (17). A mouse monoclonal antibody recognizing an epitope in the EGF receptor (EGFR; residues 996–1002) was obtained from MP Biomedicals (clone c11; Irvine, CA). A mouse monoclonal anti-erbB2 antibody directed toward the C-terminus of human c-*neu* (residues 1242–1255) was purchased from Oncogene Research Products (Ab-3; La Jolla, CA). The mouse IgM monoclonal antibody RTJ.1 recognizes the C-terminal domain of erbB3; this antibody and an isotype matched negative control clone (C48-6) was obtained from BD Biosciences PharMingen (San Diego, CA). Affinity purified rabbit polyclonal antisera for EGFR (sc-03), erbB3 (sc-285), erbB4 (sc-283), and the NRG-1 "a"-carboxy terminal domain (sc-348) were obtained from Santa Cruz Biotechnology (Santa Cruz, CA). A mouse monoclonal antibody recognizing erbB2 phosphorylated on $Tyr^{1248}$ (clone PN2A) was purchased from Lab Vision Corporation (Fremont CA). A rabbit anti-S100β polyclonal antibody (antibody Z0311) was obtained from DAKO (Glostrup, Denmark) and a mouse anti-S100β monoclonal antibody (clone 15E2-E2-A1) was purchased from Chemicon (Temecula, CA). Nonimmune mouse and rabbit IgGs were obtained from Pierce (Rockford, IL). Horseradish peroxidase (HRP)-conjugated donkey antirabbit and donkey antimouse secondary antibodies were from Jackson ImmunoResearch Laboratories, Inc. (West Grove, PA). Tyramide signal amplification reagents, including streptavidin–horseradish peroxidase, biotinyl tyramide, amplification diluent, and blocking reagent, were purchased from Perkin-Elmer Life and Analytical Science Products (Renaissance TSA-Indirect kit; Boston, MA). DAB peroxidase substrate (SK-4100) was obtained from Vector Laboratories (Burlingame, CA).

### Immunoblotting

Lysates for immunoblotting were prepared by homogenizing specimens in TRIzol reagent (Invitrogen Life Technologies, Carlsbad, CA) according to the manufacturer's protocol. Protein pellets were dissolved in 1% sodium dodecyl sulfate (SDS) supplemented with protease (Sigma #P8340) and phosphatase (Sigma #P5726) inhibitors diluted 1:100–1:250. Protein concentrations were determined with a modified Lowry method (*DC* Protein Assay; Bio-Rad, Hercules, CA), and equivalent quantities of protein lysates were resolved using 8% SDS polyacrylamide gels. Proteins were transferred to PVDF membranes by electroblotting for 180 minutes at 0.5 A in transfer buffer (25 mM Tris [pH 8.3], 0.192 M glycine, 20% methanol). Nonspecific binding was blocked by incubating membranes in 5% nonfat dry milk in TBST (0.15 M NaCl, 10 mM Tris [pH 8.0], 0.05% Tween-20) before incubation with primary antibody. The following primary antibody concentrations were used for immunoblotting: pan NRG-1 (1:5000), EGFR (sc-03; 1:1000), erbB2 (Oncogene Ab-3; 1:500), erbB3 (sc-285; 1:1000), and erbB4 (sc-283; 1:1000). Horseradish peroxidase conjugated donkey antirabbit and donkey antimouse secondary antibodies (Jackson Immunoresearch Laboratories) were used at a 1:10000 dilution in 5% nonfat dry milk/TBST. Immunoreactive species were detected by enhanced chemiluminescence (Pierce).

Schwannomas commonly show highly variable degrees of collagenization. This variability can markedly alter the relative contribution intracellular and extracellular proteins make to the final protein composition of tumor lysates. In keeping with this, our preliminary experiments demonstrated that using GAPDH, β-actin, or ERK-2 immunoreactivity as a loading control for schwannoma lysates was problematic. Consequently, we verified equivalent loading and transfer by Coomassie staining PVDF membranes posttransfer. Specificity of immunoblotting was determined in parallel experiments in which primary antibodies were preincubated with a 5- to

10-fold excess of the appropriate immunizing peptide before probing blots.

## Immunohistochemistry

Immunohistochemistry for NRG-1 and its erbB receptors was performed using a highly sensitive staining protocol we have previously developed and validated (18). In brief, after deparaffinization of 4- to 5-μm sections in xylenes and graded alcohols, antigen rescue was performed by gently boiling slides in 10 mM citrate buffer (pH 6.0) for 15 minutes and then allowing them to cool to room temperature for 15 minutes. Nonspecific binding was blocked by incubating sections for 15 minutes with TNB blocking buffer (0.1 M Tris-HCl [pH 7.5]/0.15 M NaCl/0.5% blocking reagent [Perkin-Elmer]) at room temperature. Sections were then incubated overnight at 4°C with primary antibodies diluted in blocking buffer (pan NRG-1, 1:250-1:500; EGFR [clone c11], 1:100; erbB2 [Oncogene Ab-3], 1:100; erbB3 [clone RTJ.1], 1:100; erbB4 [sc-283], 1:500; and phosphorylated erbB2 [clone PN2A], 1:500). Adjacent sections of each tumor were stained with anti-S100β antibody as a positive control. After 3 rinses in phosphate-buffered saline (PBS; 10 minutes per rinse), sections were incubated for one hour at room temperature with horseradish peroxidase-conjugated secondary antibody (diluted 1:500 in blocking buffer). After 3 washes in PBS, biotinyl tyramide (diluted 1:50 in amplification diluent) was applied to tissue sections for 10 minutes at room temperature. Sections were again washed 3 times in PBS, following which they were incubated with streptavidin-HRP (diluted 1:100 in TNB) for 45 minutes. After 3 final washes with PBS, immunoreactive structures were visualized by diaminobenzidine deposition. To confirm the specificity of staining, control sections were incubated with nonimmune rabbit or mouse immunoglobulin in place of the primary antibodies; no staining was observed in these experiments. When the immunizing peptide was available, the specificity of staining was further confirmed by preincubating antisera with either the immunizing peptide or a nonrelated peptide (10 ng/mL); in all instances, preincubation with the immunizing peptide, but not the nonrelated peptide, abolished or markedly reduced the staining pattern observed with primary antibody alone.

For double-label immunohistochemistry, sections were processed as described and incubated with a rabbit polyclonal antibody recognizing the subset of NRG-1 transmembrane precursors with an "a" variant carboxy terminus (antibody sc-348; 1:500 dilution) and a mouse anti-S100β monoclonal antibody (1:100 dilution). NRG-1-immunoreactive structures were labeled as described except that Cy3-conjugated streptavidin was used for detection rather than streptavidin-HRP. Sections were then incubated with a FITC-conjugated antimouse secondary antibody to label S100β-immunoreactive cells. After 3 PBS rinses, sections were mounted using 1:1 PBS:glycerol and examined by fluorescence microscopy.

## Reverse Transcriptase–Polymerase Chain Reaction Analyses of NRG-1 Isoforms Expressed in Schwannoma Biopsy Specimens

Our designation of NRG-1 domains follows the nomenclature of Peles and Yarden (19). The common forward oligonucleotide used for amplification of sequences encoding the EGF-like and juxtamembrane domains of NRG-1 corresponds to nucleotides 631–648 of human neu differentiation factor (NDF; GenBank accession no. U02326) (20). The reverse oligonucleotide used for PCR of NRG-1 transmembrane precursor cDNAs represents nucleotides 811–828 (encoding a portion of the transmembrane domain sequence) of human NDF. This oligonucleotide pair will amplify sequences encoding all possible combinations of EGF-like and juxtamembrane sequences found in NRG-1 transmembrane isoform mRNAs. Secreted NRG-1 isoform cDNAs were amplified using a reverse oligonucleotide corresponding to nucleotides 482–502 of a human NDFβ3 splice variant (GenBank accession no. U02327) (20) in combination with the common forward oligonucleotide.

Total RNA was isolated from schwannomas using TRIzol reagent following the manufacturer's recommendations. Single-stranded cDNA for use as a polymerase chain reaction (PCR) template was reverse transcribed from total cellular RNA in a 20-μL reaction containing random hexamer primers and Moloney murine leukemia virus reverse transcriptase (RT) (Superscript Plus; Life Technologies, Gaithersburg, MD). After completion of reactions, samples were diluted to 100 μL with distilled water, boiled for 5 minutes, and stored at –80°C until use.

Two microliters of each cDNA was used as a PCR template in reactions performed for 35 cycles of 94°C for one minute, 55°C for one minute, and 72°C for 2 minutes. PCR products were ligated to pCR4-TOPO and ligations transformed into *Escherichia coli* (TOP10 strain) as recommended by the manufacturer (Invitrogen). The sequence of these clones was determined by cycle sequencing using an automated sequencer (ABI Model 373A DNA Sequencing System; Applied Biosystems, Inc., Foster City, CA).

## Real-Time Quantitative Reverse Transcriptase–Polymerase Chain Reaction

One microgram of total RNA isolated from normal nerve or schwannomas as described was reverse-transcribed in a 20-μL reaction containing random hexamer primers and Moloney murine leukemia virus RT; a parallel reaction, performed identically except for the addition of RT, was used to verify an absence of genomic DNA contamination. After completion of RT, samples were diluted to 100 μL with distilled water, boiled for 5 minutes, and stored at –80°C until used in real-time PCR experiments.

Real-time quantitative PCR was performed using an ABI 7500 Real Time PCR System (Applied Biosystems, Inc.). Assays for NRG-1, NRG-2, and erbB cDNA levels were performed using TaqMan MGB probes labeled with FAM dye (ABI Assay-on-Demand Gene Expression assays) in a 20-μL reaction containing 2 μL of cDNA, ROX passive reference dye, and TaqMan Universal PCR mix (Applied Biosystems, Inc.); this reaction mix was supplemented with uracil N-glycosylase to minimize the possibility that spurious results could be produced by carryover of contaminating PCR products. The specific primer sets used and the regions hybridizing to the FAM-labeled probes are as follows:

1. EGFR: Hs00193306_m1, probe sequence starts at nucleotide 2715 of NM005228.
2. ErbB2: Hs00170433_m1, probe sequence starts at nucleotide 2139 of NM004448.
3. ErbB3: Hs00176538_m1, probe sequence starts at nucleotide 273 of NM001982.
4. ErbB4: Hs00171783_m1, probe sequence starts at nucleotide 1524 of NM005235.
5. NRG-1α: Hs01103794_m1, probe hybridizes to sequences at the junction of the EGF-like common and α domains.
6. NRG-1β: Hs00247624_m1, probe hybridizes to sequences at the junction of the EGF-like common and β domains.
7. NRG-1 class I/II isoforms: Hs00247620_m1, probe and amplicon are within sequences encoding the immunoglobulin-like domain.
8. NRG-1 class III isoforms: Hs00247641_m1, probe hybridizes to sequences at the junction of the SMDF amino terminal and EGF-like common domains.
9. NRG-2α: Hs00993410_m1, probe hybridizes to sequences at the junction of the EGF-like common and α domains.
10. NRG-2β: Hs00993401_m1, probe hybridizes to sequences at the junction of the EGF-like common and β domains.

Levels of 18S ribosomal cDNA were assayed in parallel reactions using TaqMan MGB probes labeled with VIC dye (Applied Biosystems 4319413E). Assays for 18S and target transcripts were performed in triplicate for each cDNA.

Experimental results were analyzed using Applied Biosystems Sequence Detection Software (version 1.3.1.22). The relative quantity of each target transcript was established by normalizing the level of the corresponding cDNA to that of 18S cDNA in the same RT reaction. Controls lacking added template were performed in parallel with each primer set to verify an absence of contamination.

### Reverse Transcriptase–Polymerase Chain Reaction Analyses of NRG-3, NRG-4, and Epidermal Growth Factor Family Ligand Expression in Schwannomas

One microgram of total RNA isolated from schwannomas as described was reverse transcribed in a 20-μL reaction containing oligo-dT primer and Moloney murine leukemia virus RT; a parallel reaction, performed identically except for the addition of RT, was used to verify an absence of genomic DNA contamination. Two microliters of each cDNA was used as a PCR template in reactions performed for 35 cycles of 94°C for one minute, 55°C for one minute, and 72°C for 2 minutes. The sequences of the primers used in these experiments correspond to the following nucleotides of the indicated archived sequences:

1. NRG-2: 926–949 and 1251–1230, GenBank accession no. NM013984.
2. NRG-3: 169–189 and 607–587 (set 1); 79–102 and 529–510 (set 2), GenBank accession no. AK098823.
3. NRG-4: 66–87 and 475–453, GenBank accession no. NM138573.
4. Heparin-binding EGF: 753–776 and 1158–1135, GenBank accession no. NM001945.
5. Betacellulin: 279–298 and 740–717, GenBank accession no. NM001729.
6. Epiregulin: 2548–2571 and 3071–3049, GenBank accession no. NM001432.
7. Epidermal growth factor: 3288–3311 and 3690–3671, GenBank accession no. NM001963.
8. Transforming growth factor α: 881–897 and 1348–1325, GenBank accession no. NM003236.
9. Amphiregulin: 574–597 and 1010–990 (set 1); 103–126 and 614–591 (set 2), GenBank accession no.NM001657.

PCR products were resolved on 1.5% agarose gels and visualized by ethidium bromide staining. Parallel reactions lacking cDNA were performed to verify an absence of contamination in these experiments.

## RESULTS

### Human Schwannomas Express Multiple NRG-1-Immunoreactive Proteins

At least 15 structurally distinct NRG-1 proteins are produced from a single gene through a combination of alternative mRNA splicing and alternative promoter use (21). All of these proteins contain an EGF-like domain that directly binds to and activates NRG-1 receptors (22). We therefore focused initially on determining whether the NRG-1 EGF-like domain was detectable in human schwannomas. Lysates prepared from 6 surgically resected human schwannomas (Table 1) were immunoblotted and probed using a "pan NRG-1" antibody that recognizes the amino terminal (common) portion of the NRG-1 EGF-like domain. Multiple NRG-1-immunoreactive species were detectable in all 6 schwannomas with sizes ranging from 150 to 58 kD (Fig. 1A). The masses of the larger (150 and 120 kD) NRG-1 proteins labeled by this antibody were similar to those of the NRG-1 isoforms we have previously detected in brain and spinal cord lysates (17) and likely represent NRG-1 transmembrane precursor proteins. The other NRG-1-immunoreactive species detectable in schwannomas (90, 65, 60, and 58 kD polypeptides) were too small to be transmembrane precursors and had masses consistent with either directly secreted NRG-1 isoforms or extracellular domain sequences released by proteolytic cleavage of NRG-1 transmembrane precursors (17, 21, 23). Comparing the NRG-1 proteins detected in schwannomas with those evident in normal eighth cranial nerve, we found that the most prominent (58 kD) NRG-1 protein in normal nerve comigrated with

**TABLE 1.** Characteristics of Human Schwannomas Used for Protein and RNA Analyses

| Case No. | Diagnosis | Location | Age/Race/Gender |
|---|---|---|---|
| 1 | Schwannoma | Sacral spinal nerve | 48/H/M |
| 2 | Schwannoma | Sacral spinal nerve | 31/H/F |
| 3 | Schwannoma | Vestibular nerve | 35/W/F |
| 4 | Schwannoma | Thoracic spinal nerve | 31/W/F |
| 5 | Schwannoma | Vestibular nerve | 38/W/F |
| 6 | Schwannoma | Thoracic spinal nerve | 22/B/F |

H, hispanic; W, white; B, black.

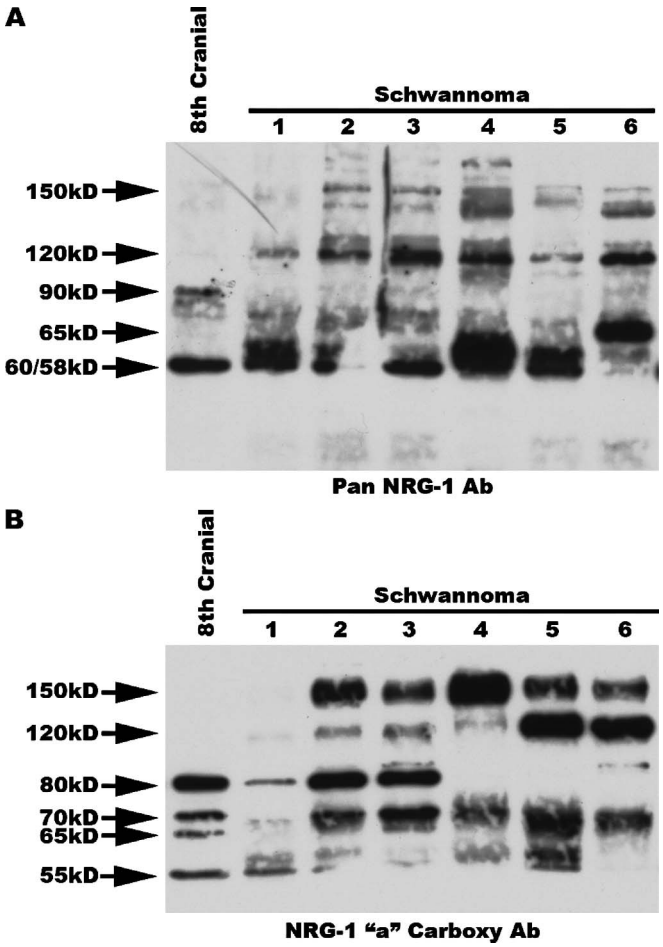


**FIGURE 1.** Multiple NRG-1-immunoreactive species are expressed in human schwannomas. **(A)** Lysates of normal eighth cranial nerve and 6 schwannomas probed with a ''pan-NRG-1'' antibody recognizing the epidermal growth factor-like common domain found in all NRG-1 isoforms. **(B)** An antibody recognizing the ''a'' variant carboxy terminus, a domain found in a major subset of NRG-1 transmembrane precursors, recognizes multiple proteins in human schwannomas and eighth cranial nerve. Arrows to the left of these 2 panels indicate the immunoreactive species and their molecular weights. Numbers above each schwannoma lane correspond to the cases indicated in Table 1.

a protein present in the majority of the schwannomas tested. However, schwannomas also consistently demonstrated prominent expression of several higher-molecular-weight NRG-1 isoforms that were detectable in normal nerve only with long exposures, suggesting that the tumors expressed distinct profiles of NRG-1 isoforms. In both schwannomas and eighth cranial nerve, labeling of NRG-1-immunoreactive proteins was abolished or markedly diminished by preincubating the primary antibody with immunizing peptide (data not shown).

To further establish the identity of the proteins labeled by the pan NRG-1 antibody, schwannoma lysates were probed with an antibody that recognizes an epitope within the carboxy terminus of a major subset of NRG-1 isoforms (transmembrane precursors with an "a" variant carboxy terminus). This antibody labeled several proteins in schwannomas that ranged in size from 55 to 150 kD (Fig. 1B). The larger polypeptides detected by the "a" carboxy terminus antibody (150 and 120 kD) comigrate with the larger species labeled by the pan NRG-1 antibody, consistent with the notion that these molecules are NRG-1 transmembrane precursors. The anti-NRG-1 "a" carboxy terminus antibody also labeled several smaller proteins in the eighth cranial nerve and in a subset of schwannomas. These smaller (80, 70, 65, and 55 kD) proteins are too small to be full-length NRG-1 transmembrane precursor proteins and likely represent proteolytic cleavage products of NRG-1 transmembrane precursors. Labeling of all of the polypeptides detected by the anti-"a" carboxy terminus antibody in schwannomas and the eighth cranial nerve was abolished or markedly diminished by preincubating the primary antibody with immunizing peptide (data not shown). Considered together, these findings indicate that multiple NRG-1 proteins are present in schwannomas, at least some of which are NRG-1 transmembrane precursors.

NRG-1 protein in schwannomas could be primarily associated with neoplastic Schwann cells or alternatively be derived from nonneoplastic elements within the tumors (e.g. vasculature or cells in the tumor capsule). To establish the distribution of NRG-1 in schwannomas, we immunostained paraffin sections prepared from a second series of 6 tumors (Table 2) using the pan NRG-1 antibody. NRG-1 immunoreactivity was readily detectable in 4 of these neoplasms (Fig. 2A, B). Immunostaining of neoplastic Schwann cells was eliminated when the pan NRG-1 antibody was replaced with nonimmune rabbit IgG (Fig. 2C) and was markedly

**TABLE 2.** ErbB and NRG Immunoreactivity in Human Schwannomas

| Case No. | Location | Age/Race/Gender | ErbB-1 | ErbB-2 | ErbB-3 | ErbB-4 | PN2A |
|---|---|---|---|---|---|---|---|
| 7 | Vestibular nerve | 37/W/F | + | + | + | + | − |
| 8 | Thoracic spinal nerve | 22/B/F | − | + | − | − | + |
| 9 | Thoracic spinal nerve | 71/W/M | + | + | + | − | + |
| 10 | Thoracic spinal nerve | 71/W/M | + | + | + | − | − |
| 11 | Vestibular nerve | 74/W/F | − | + | − | − | + |
| 12 | Vestibular nerve | 57/B/M | − | + | + | + | + |

W, white; B, black.

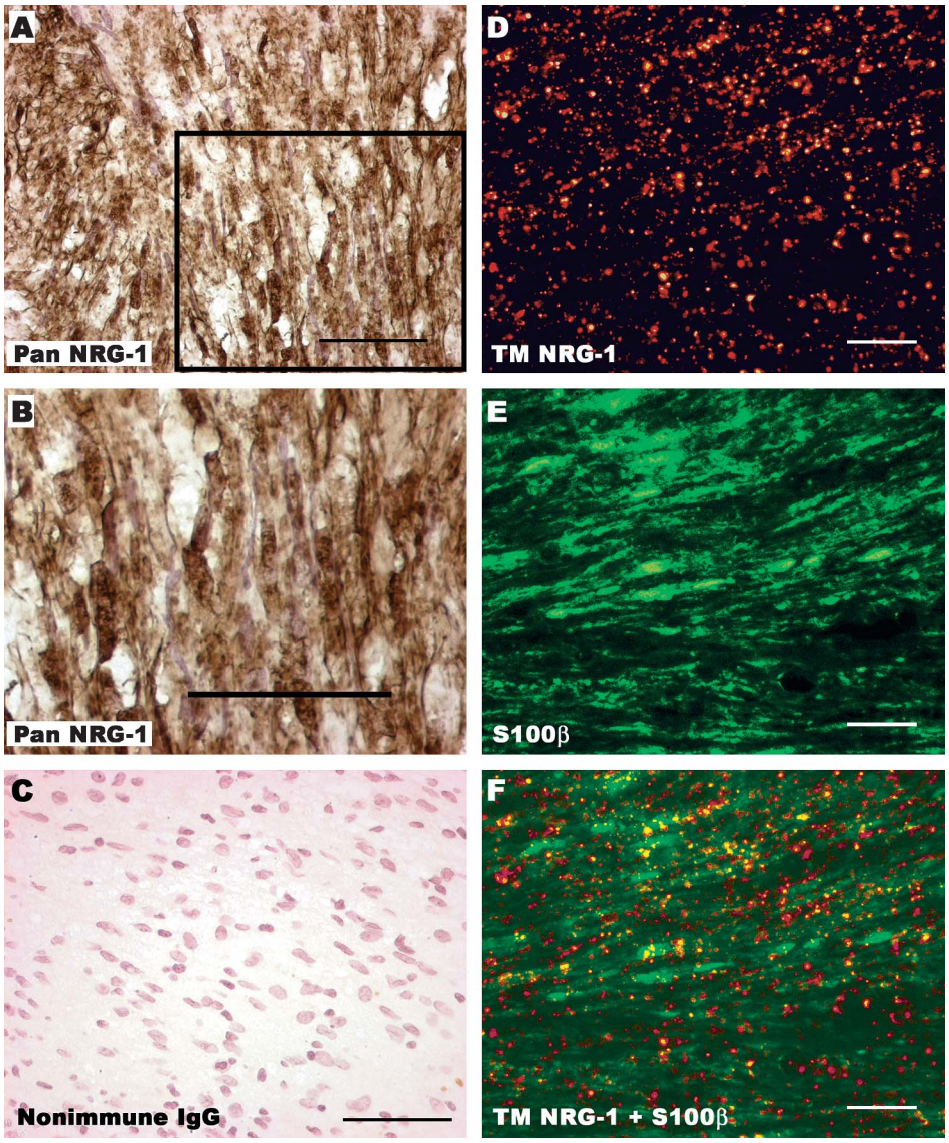


**FIGURE 2.** Immunohistochemical demonstration of NRG-1 like protein expression in a human schwannomas. **(A)** Section stained with the pan NRG-1 antibody. **(B)** Enlarged view of the area indicated by the box in **(A)**. **(C)** Replacing the pan NRG-1 antibody with nonimmune IgG abolishes this staining. Sections illustrated in **(A–C)** have been lightly counterstained with hematoxylin. **(D–F)** Double-label immunofluorescence in a human schwannoma immunostained for NRG-1 transmembrane precursors with an ''a'' variant carboxy terminus **(D)** and S100β **(E)**. These images are merged in panel **(F)**. Scale bars = 50 μm.

diminished when the primary antibody was preincubated with the immunizing peptide before staining tumor sections.

To determine whether NRG-1 immunoreactivity was associated with neoplastic Schwann cells in schwannomas, double-label immunohistochemistry was performed using the anti-"a" carboxy terminus rabbit polyclonal antibody in combination with a mouse anti-S100β monoclonal antibody. Immunoreactivity for this subset of NRG-1 proteins was evident as punctuate staining scattered diffusely throughout schwannomas (Fig. 2D). A comparison of the distribution of NRG-1 and S100β immunoreactivity showed that these antigens extensively colocalized within the tumors (Fig. 2E, F). Because the epitope recognized by the anti-"a" carboxy terminus antibody is not thought to be released from cells synthesizing NRG-1 transmembrane precursors, these findings also suggest that neoplastic Schwann cells within schwannomas are the source of at least a portion of the NRG-1 protein detectable in these peripheral nerve sheath tumors.

## Schwannomas Overexpress a Complex Mixture of α and β Transmembrane Precursors From the Class II and Class III NRG-1 Subfamilies

The presence of multiple, variably sized NRG-1 proteins in schwannomas suggested that these tumors express several structurally and functionally distinct NRG-1 isoforms. Structural variation in the NRG-1 EGF-like domain and adjacent regions has particularly important functional implications. The NRG-1 EGF-like domain is composed of an invariant amino terminal (common) domain that can be fused to either an α or a β domain (Fig. 3), resulting in the production of isoforms that differ in their affinity for the NRG-1 receptors and in their ability to elicit at least some responses such as mitogenesis (21). A structurally variable juxtamembrane domain is found immediately carboxy terminal to the EGF-like domain; one variant of this domain ("3" isoforms) contains a termination codon and thus allows the protein to be directly secreted,

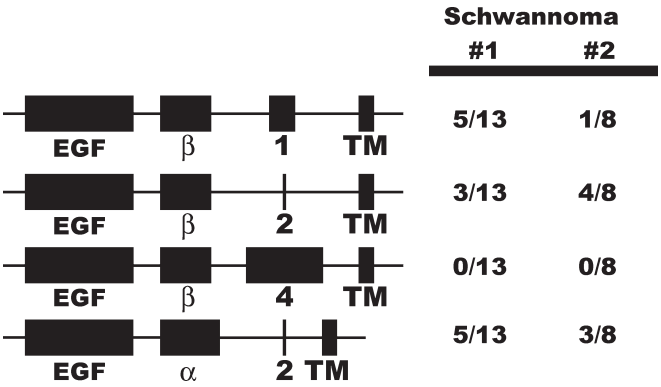


**FIGURE 3.** Schwannomas express mRNAs encoding a complex mixture of α and β NRG-1 isoforms. Structural diagrams of the protein structures predicted by partial NRG-1 cDNAs isolated from schwannomas are indicated to the left. Boxes in these structural diagrams indicate each protein domain, with the size of the box being directly proportional to the size of that domain; lines connecting boxes are included only to indicate structural linkage between domains. Domains are as follows: EGF, the NRG-1 EGF-like common domain; α or β, NRG-1 EGF-like α or β variant domains; 1, 2, or 4 variant juxtamembrane domains; transmembrane, the initial portion of the transmembrane domain of NRG-1 transmembrane precursor proteins. Ratios indicated adjacent to each juxtamembrane domain indicate the frequency with which clones encoding that structural variant were identified when polymerase chain reaction-generated clones were sequenced.

whereas the other 3 (1, 2, or 4 variants) are fused to membrane-spanning sequences in NRG-1 transmembrane precursors (Fig. 3). To determine whether the NRG-1 isoforms expressed in human schwannomas demonstrated structural variability in these regions, we used RT-PCR to amplify sequences encoding the EGF-like common, EGF-like variant, juxtamembrane, and transmembrane domains of NRG-1 transmembrane precursors. Using RNA isolated from 5 of the same tumors used for our immunoblot analyses, we found that these NRG-1 sequences were uniformly detectable in all 5 schwannomas (data not shown). To further examine the structure of these NRG-1 transmembrane precursor mRNAs, we cloned the PCR products derived from 2 tumors and sequenced 21 independent subclones. We found that the NRG-1 transmembrane precursor transcripts expressed in schwannomas were structurally diverse and included mRNAs encoding NRG-1 α2, β1, and β2 isoforms (Fig. 3). Using these same schwannoma cDNA templates, we also attempted to amplify sequences encoding the EGF-like common, EGF-like variant, and "3" juxtamembrane domains of directly secreted NRG-1 isoforms. Although these primers produced a PCR product of the expected size from control templates, we could not detect secreted NRG-1 isoform transcripts in any of the 5 schwannomas tested (data not shown).

The NRG-1 protein we detected in a normal eighth cranial nerve and schwannomas by immunoblot analyses is potentially produced by cells endogenous to both tissue types. However, it is known that NRG-1 protein is transported anterogradely and retrogradely along axons in peripheral nerve (24), raising the question of whether much of the NRG-1 protein we detected in the eighth cranial nerve was axon-derived. Because mRNAs are largely excluded from axons, measurements of NRG-1 mRNA levels are likely to produce a more accurate comparison of the levels of NRG-1 expression per cell in normal and neoplastic Schwann cells. We therefore compared the levels of NRG-1 α and β transcripts in normal nerves and schwannomas arising from these same nerves. Performing real-time quantitative PCR with TaqMan primers specific for NRG-1α or NRG-1β cDNAs and normalizing the resulting data to the levels of 18S ribosomal RNA present in the same cDNAs, we found that both types of transcripts were detectable in the normal eighth cranial nerve and spinal nerve root. The expression of NRG-1α mRNA was elevated in 4 of the 5 schwannomas (Fig. 4A), being found at levels ranging from 1.6 to over 4,000 times greater than that found in normal nerve. NRG-1β mRNA expression was increased in all 5 of the schwannomas we tested (Fig. 4B), with levels varying from 4.3- to 312-fold greater than those present in normal nerve.

Three major NRG-1 subfamilies (class I [neu differentiation factor (NDF)], class II [GGF], and class III [sensory and motor neuron-derived factor (SMDF)/cysteine-rich domain] isoforms) have been identified, each of which is characterized by subfamily-specific amino terminal sequences with distinct functional characteristics. To determine which of these 3 subfamilies are expressed in schwannomas, we performed RT-PCR analyses using primers specific for the amino terminal sequences of each subfamily. We found that class II and class III transcripts were readily detected in schwannomas, whereas class I mRNA expression was not evident in these tumors (data not shown). To compare the relative levels of expression of the major NRG-1 subfamilies in schwannomas with that in normal eighth cranial nerve, we performed real-time quantitative PCR using TaqMan primers specific for the immunoglobulin-like (Ig-like) domain present in class II isoforms or primers specific for the class III amino terminal domain. Again, we found that both primer sets detected these mRNAs in normal nerve. The expression of class II NRG-1 mRNA was consistently increased in the 5 schwannomas we examined (Fig. 4C), with levels ranging from 1.3- to 137-fold greater than that found in normal nerve. Class III NRG-1 transcript levels were likewise elevated in 4 schwannomas (Fig. 4D), with levels 3.2- to 1430-fold higher than the levels detected in normal nerve. We conclude that human schwannomas overexpress a complex mixture of NRG-1 mRNAs encoding α and β transmembrane precursors from the class II and III subfamilies.

## A Subset of Schwannomas Overexpress NRG-2 α and β Isoforms

Neuregulin-2 (NRG-2 [25, 26]; also known as *Don-1* [27] and neural- and thymus-derived activator for erbB kinases (NTAK [28]) is a NRG-1-related growth factor represented by 6 alternatively spliced isoforms derived from a single gene. NRG-2 is heparin-binding (28) and stimulates phosphorylation of the NRG-1 receptor subunits erbB2, erbB3, and erbB4 (25–28). Because these features are shared with the GGF-like activity previously identified in human schwannomas (13), we examined the potential expression of NRG-2 transcripts in the

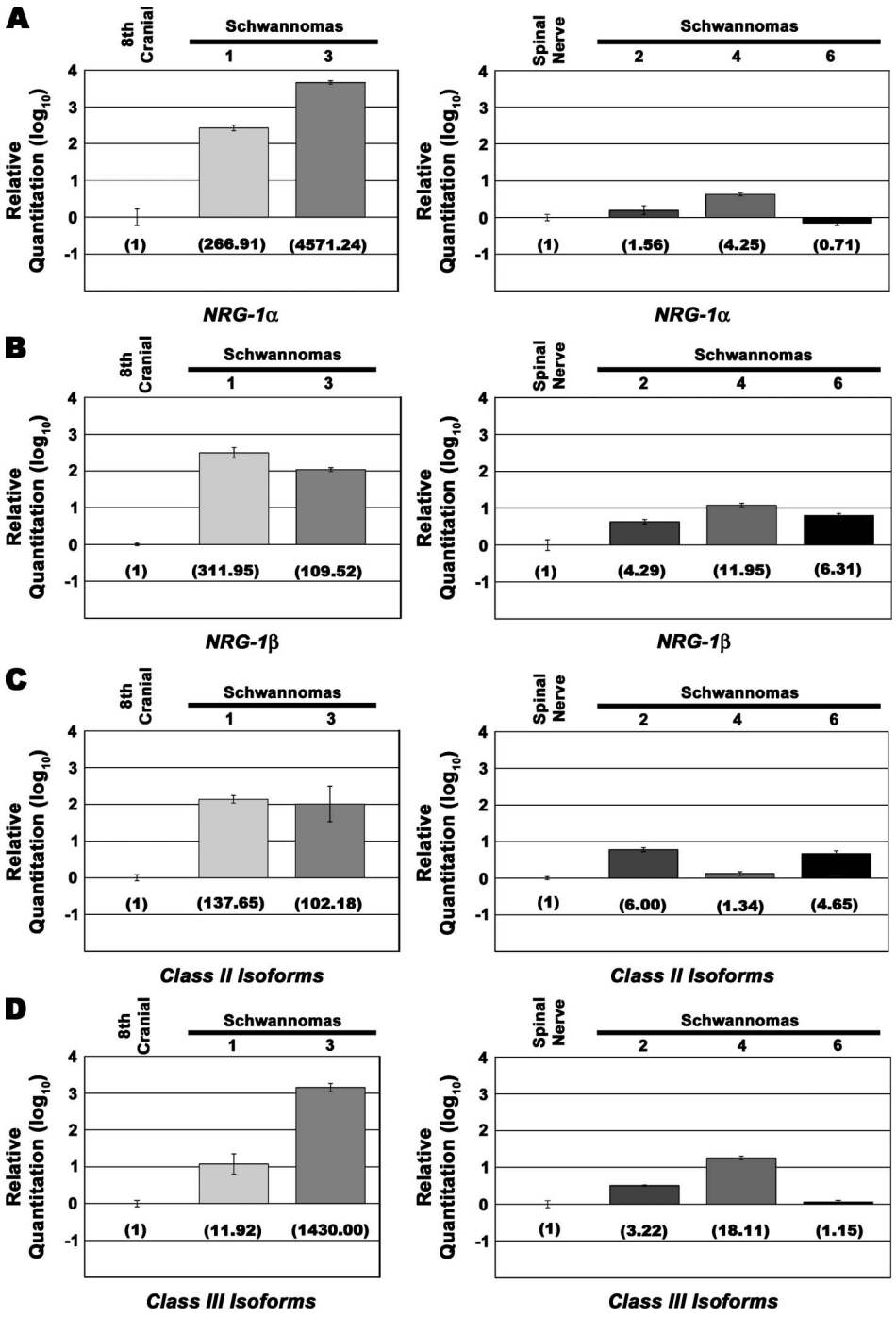


**FIGURE 4.** Real-time quantitative polymerase chain reaction assays for mRNAs encoding specific NRG-1 isoforms in schwannomas and normal nerve. Comparison of the levels of mRNAs encoding NRG-1α **(A)**, NRG-1β **(B)**, class II isoforms **(C)**, and class III isoforms **(D)** in human schwannomas and their nerve of origin (normal eighth cranial [left panels] or normal spinal nerve root [right panels]). **(A–D)** Bars indicate the relative levels of expression, with expression in normal nerve arbitrarily designated as 1; note that the values indicated by the bars are expressed on a $\log_{10}$ scale. Ninety-five percent confidence intervals are indicated for each bar. Numbers in parentheses below the bars indicate the fold change converted from $\log_{10}$. The designation of each schwannoma corresponds to the case numbers indicated in Table 1.

same 5 schwannomas described above. In initial RT-PCR experiments performed using primers specific for amino terminal domain sequences present in all NRG-2 isoforms, we readily detected NRG-2 mRNA in all 5 schwannomas (data not shown). To compare the levels of expression of NRG-2 transcripts in schwannomas with that in normal nerve, we then quantitated the levels of NRG-2 mRNA in these tissues. Because the EGF-like domain of NRG-2, like that of NRG-1, is alternatively spliced to produce isoforms with distinct effects on cell growth and erbB phosphorylation (29), we performed these analyses using real-time PCR with TaqMan primers specific for NRG-2α or NRG-2β cDNAs and normalized the resulting data to the levels of 18S ribosomal RNA present in the same RT reactions. We found that the expression of NRG-2α was elevated in 3 of 5 schwannomas with levels of mRNA 1.8- to 10.0-fold higher than the levels found in normal nerve (Fig. 5). The expression of NRG-2β transcripts was likewise upregulated 1.7- to 5.3-fold relative to normal nerve in the same 3 schwannomas that overexpressed NRG-2α mRNA.

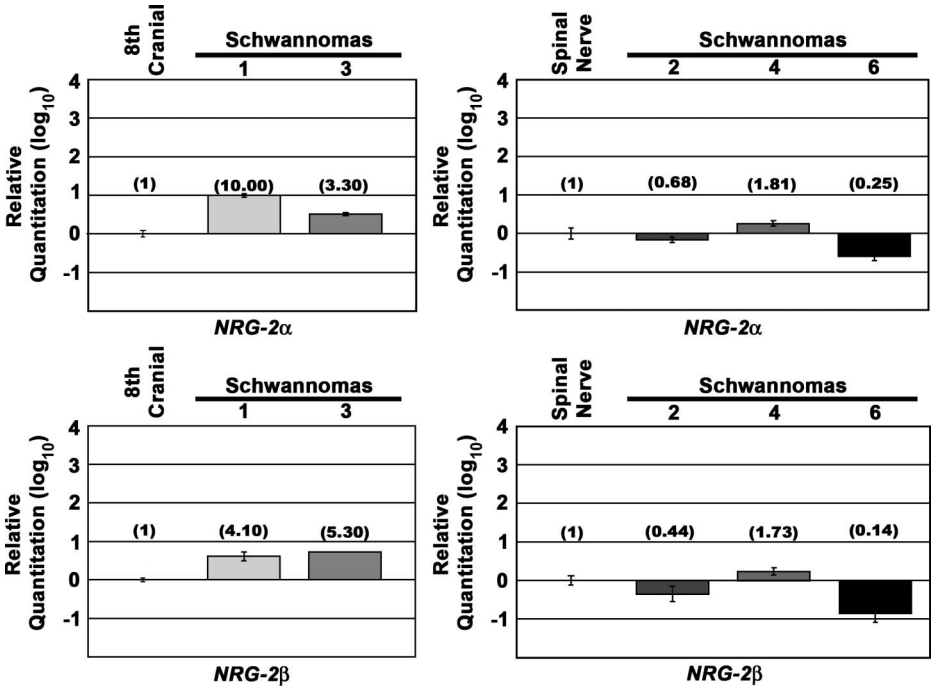


**FIGURE 5.** Real-time quantitative polymerase chain reaction assays comparing the level of expression of mRNAs encoding NRG-2α (top panel) and β (bottom panel) isoforms in human schwannomas and their nerve of origin. Bars indicate the relative levels of expression with expression in normal nerve arbitrarily designated as 1; note that these are values are expressed on a $log_{10}$ scale. Ninety-five percent confidence intervals are indicated for each bar. Numbers in parentheses below the bars indicate the fold change converted from $log_{10}$. The designation of each schwannoma corresponds to the case numbers indicated in Table 1.

## Expression of Other NRG and Epidermal Growth Factor Family Ligands in Human Schwannomas

The expression of erbB4 and EGFR in smaller subsets of schwannomas (see subsequently) raised the question of whether other NRG and EGF family ligands capable of activating these receptors might be expressed in schwannomas. To test this hypothesis, we used RT-PCR to amplify sequences encoding neuregulin-3 (NRG-3), neuregulin-4 (NRG-4), heparin-binding EGF (HB-EGF), betacellulin, epiregulin, EGF, transforming growth factor-α (TGFα), and amphiregulin. Transcripts encoding HB-EGF and epiregulin, 2 ligands capable of activating either erbB4 or EGFR, were evident in 4 of the 5 schwannomas (Fig. 6). We also found evidence that the EGFR ligand TGFα was expressed in all 5 of these tumors. In contrast, mRNAs for NRG-3, NRG-4, betacellulin, EGF, or amphiregulin were undetectable in all of the schwannomas we examined.

## Schwannomas Express Multiple ErbB Kinases and Demonstrate Constitutive Activation of ErbB Signaling

NRG-1 and NRG-2 bind directly to the erbB3 and erbB4 membrane tyrosine kinases and subsequently induce heterodimerization with erbB2 or, alternatively, in the case of erbB4, homodimerization to form active signaling complexes (30, 31). To determine whether human schwannomas express the erbB receptors necessary for responsiveness to NRG-1 or NRG-2, we immunoblotted lysates of the same schwannomas examined for NRG-1 expression (Table 1) and probed these immunoblots with antibodies recognizing erbB2, erbB3, or erbB4. ErbB2 and erbB3 were the most commonly expressed erbB kinases in schwannomas, with a protein of the expected 185 kD size being detected in all 6 schwannomas by the anti-erbB2 and anti-erbB3 antibodies (Fig. 7). Expression of erbB4 was more restricted, with an erbB4-immunoreactive protein being readily identifiable in 3 of the 6 schwannomas. The erbB2-, erbB3-, and erbB4-like immunoreactive polypeptides found in schwannomas comigrated with erbB proteins detected by these antibodies in normal eighth cranial nerve (Fig. 7 and longer exposures of these same blots [data not shown]). We conclude that one or more cell type within schwannomas

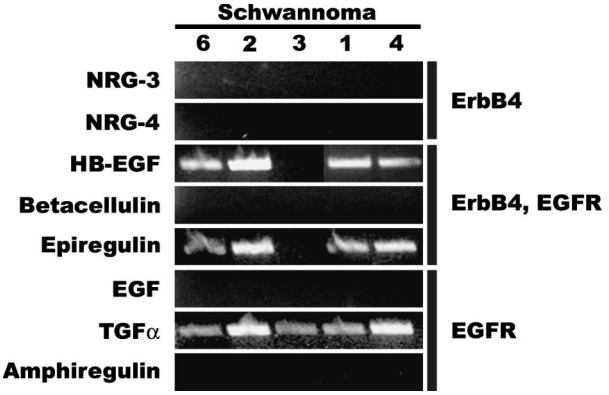


**FIGURE 6.** Reverse transcription–polymerase chain reaction analyses of the expression of mRNAs encoding NRG-3, NRG-4, and multiple EGF family ligands in human schwannomas. The identity of each ligand is indicated to the left of the corresponding panel. Numbers above each lane indicate the case number corresponding to the clinical information presented in Table 1. Thick bars to the right of the panels indicate the receptors capable of binding each ligand. HB-EGF, heparin-binding epidermal growth factor; EGF, epidermal growth factor; TGFα, transforming growth factor α.

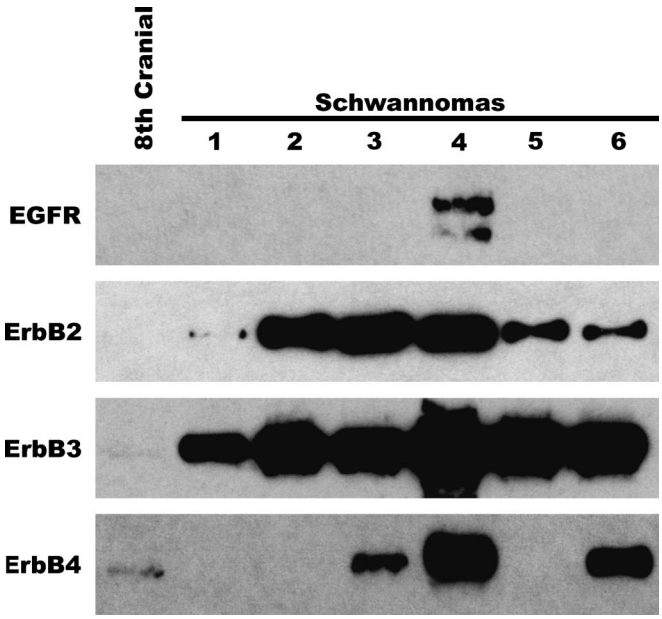


**FIGURE 7.** Western blot analyses of erbB expression in schwannomas. The specific erbB receptor examined is indicated to the left of each blot. Numbers above each schwannoma lane correspond to the cases indicated in Table 1. Longer exposures of the epidermal growth factor receptor and erbB2 blots demonstrated the presence of relatively low level of each of these receptors in normal eighth cranial nerve (data not shown).

expresses the complement of erbB receptors required for responsiveness to NRG-1 and NRG-2.

The EGF receptor (EGFR, also known as erbB1) is capable of heterodimerizing with and "crosstalking" to the NRG-1 receptors. Furthermore, expression of the EGFR is increased in other types of peripheral nerve sheath tumors (32), including a subset of malignant peripheral nerve sheath tumors (33). To determine whether EGFR expression is similarly inappropriately expressed in schwannomas, we also probed normal eighth cranial nerve and schwannoma lysates with an anti-EGFR antibody. With long exposures, a protein of the expected 170-kD size was weakly detectable in normal eighth cranial nerve using this antibody (data not shown). However, only one of the 6 schwannomas tested expressed detectable levels of EGFR protein (Fig. 7).

Our immunoblot analyses indicated that erbB2 and erbB3 (and less frequently, erbB4) were expressed in schwannomas. To determine whether the expression of erbB mRNAs was increased in schwannomas relative to their nerves of origin, we performed real-time quantitative PCR assays on normal eighth cranial nerve, normal spinal nerve, and schwannoma cDNAs using TaqMan primer sets specific for each erbB kinase. The levels of erbB transcripts established in these assays were normalized to the levels of 18S ribosomal RNA in the same cDNA. As shown in Figure 8, all 4 transcripts were present to varying degrees in normal nerve and in all of the tested schwannomas. Levels of erbB2 mRNA were elevated in 4 of the schwannomas relative to normal nerve (1.6- to 23-fold; Fig. 8B), with increased levels of erbB3 mRNA evident in 2 tumors (Fig. 8C). Paradoxically, the expression of erbB4 transcripts was lower in all 5 schwannomas than in normal nerve; we did note, however, that erbB4 mRNA accumulated to relatively higher levels in the 3 schwannomas with the highest levels of erbB4 protein by immunoblot (tumors 3, 4, and 6; Fig. 8D). The expression of EGFR messenger RNA in schwannomas was lower or equivalent to that observed in normal nerve in nearly all tumors with only one schwannoma (4, the same tumor that exhibited increased levels of EGFR protein in immunoblot analyses) showing a very slight increase in EGFR mRNA levels (Fig. 8A).

To establish whether expression of specific erbB kinases was associated with neoplastic Schwann cells, we immunostained sections of the same schwannomas examined for NRG-1 expression (Table 2) using antibodies recognizing EGFR, erbB2, erbB3, or erbB4. Focal immunoreactivity for EGFR was found in 3 of the 6 tumors, being evident as cytoplasmic staining associated with patches of tumor cells (Fig. 9A). In contrast, strong erbB2 immunoreactivity was associated with the membranes and cytoplasm of tumor cells throughout all 6 of the tumors (Fig. 9B). The anti-erbB3 mouse monoclonal antibody RTJ.1 similarly produced strong staining of the membranes and cytoplasm of tumor cells in 4 of the 6 neoplasms (Fig. 9C). An anti-erbB4 rabbit polyclonal antiserum labeled tumor cells in 2 schwannomas (Fig. 9D), but did so with a pattern distinct from that seen with the other 3 anti-erbB antibodies. ErbB4 immunoreactivity in tumor cells was prominently associated with tumor cell nuclei as well as the cytoplasm and membranes of these cells; the presence of nuclear erbB4 immunoreactivity in schwannoma cells is consistent with previous reports demonstrating that erbB4 can be proteolytically cleaved and its carboxy terminus translocated into the nucleus (31). In all instances, replacing the primary antibody with nonimmune immunoglobulin or, when possible, preincubating the primary antibody with the immunizing peptide abolished erbB immunoreactivity in schwannomas.

ErbB2 is the preferred dimerization partner for all other erbB receptors. Dimerization is accompanied by phosphorylation of multiple tyrosine residues in the carboxy terminal sequences of erbB2, including $Tyr^{1248}$, a residue whose phosphorylation is linked to activation of the ERK/MAP kinase-signaling pathway. To determine whether erbB signaling is constitutively activated in schwannomas, we immunostained sections of these tumors with PN2A, a mouse monoclonal antibody that recognizes erbB2 phosphorylated on $Tyr^{1248}$. PN2A immunoreactivity was readily identified in 4 of the 6 schwannomas, producing a punctate pattern of cytoplasmic staining in a major subset of tumor cells (Fig. 9E) that was not evident when the primary antibody was replaced with nonimmune IgG (Fig. 9F). We conclude that erbB signaling is constitutively activated in at least some schwannomas.

## DISCUSSION

There is extensive evidence indicating that inactivating and missense mutations of the *NF2* tumor-suppressor gene play a key role in the pathogenesis of schwannomas. We have hypothesized that inappropriate signaling by as yet unknown

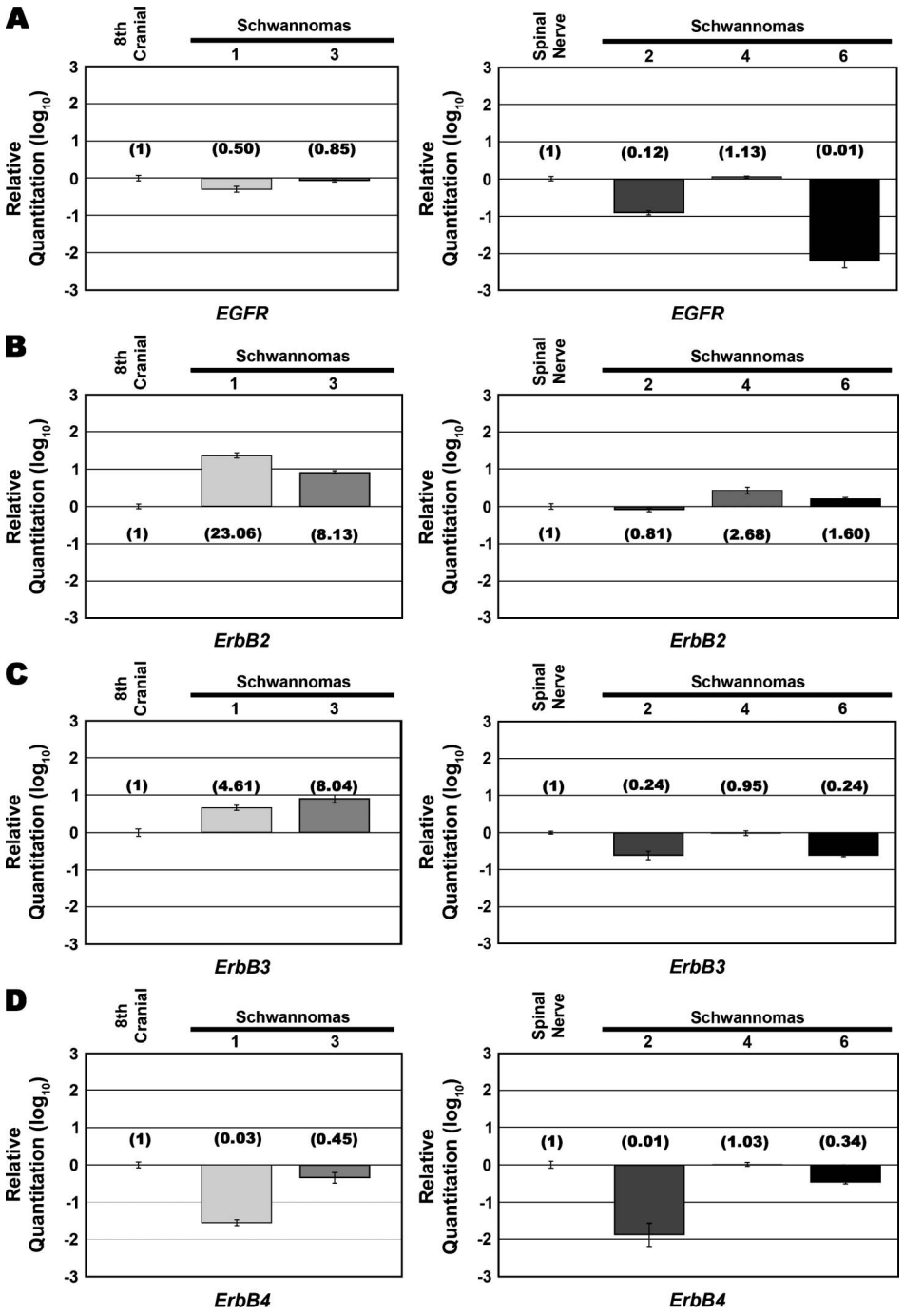


**FIGURE 8.** Real-time quantitative polymerase chain reaction comparing the levels of expression of epidermal growth factor receptor, erbB2, erbB3, and erbB4 mRNAs in schwannomas to that detectable in normal nerve. Bars indicate relative levels of expression, with expression in normal nerve arbitrarily designated as 1; note that these are values are expressed on a $\log_{10}$ scale. Ninety-five percent confidence intervals are indicated for each bar. Numbers in parentheses below the bars indicate the fold change converted from $\log_{10}$. The designation of each schwannoma corresponds to the case numbers indicated in Table 1.

growth factors also contributes to this process and, based on the results presented here, propose that NRG-1 and/or NRG-2 proteins are among the growth factors promoting schwannoma tumorigenesis. In support of this hypothesis, we have found that neoplastic Schwann cells within schwannomas express multiple α and β transmembrane precursors from the class II and III NRG-1 subfamilies as well as NRG-2 α and β isoforms. Furthermore, schwannomas express transcripts encoding NRG isoforms at levels much higher than those found in normal nerve. We have also found that schwannomas consistently express erbB2 and erbB3, 2 receptor tyrosine kinases that mediate NRG-1 and NRG-2 responses. These observations, considered together with our demonstration of constitutive erbB2 phosphorylation in schwannomas, are consistent with the hypothesis that autocrine, paracrine, and/or juxtacrine NRG-1 and/or NRG-2 signaling in neoplastic Schwann cells promotes schwannoma tumorigenesis. Our results also raise intriguing questions about the role specific NRG-1 and NRG-2 isoforms play in this process, how NRG-1 and NRG-2 actions in schwannomas differ from the actions of

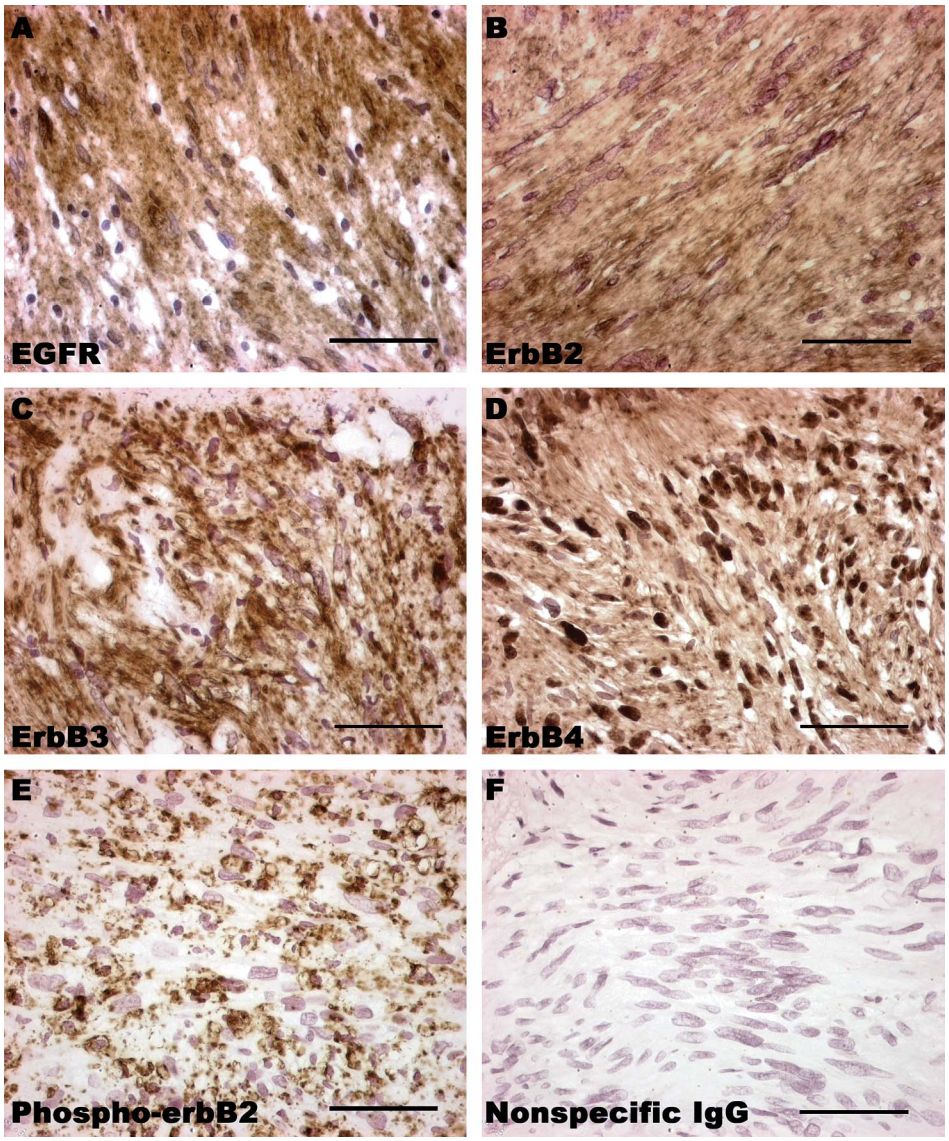


**FIGURE 9.** Representative sections of human schwannomas immunostained for epidermal growth factor receptor (EGFR) **(A)**, erbB2 **(B)**, erbB3 **(C)**, erbB4 **(D)**, or erbB2 phosphorylated on residue 1248 ($pTyr^{1248}$; **[E]**). Staining for each of these antigens was abolished in control sections in which the primary antibody was replaced with nonimmune mouse antibody (EGFR, $pTyr^{1248}$) or IgM nonspecific control antibody (erbB3) or when the primary antibody was preincubated with the immunizing peptide (erbB2, erbB4); an example of this is indicated in the last panel **(F)**. All sections have been lightly counterstained with hematoxylin. Scale bar = 50 μm.

these same growth factors in other types of peripheral nerve sheath tumors such as neurofibromas and malignant peripheral nerve sheath tumors (MPNSTs), and the potential for interactions between NRG-1/NRG-2 signaling and signaling by other erbB ligands expressed in schwannomas.

Our real-time quantitative PCR analyses indicate that schwannomas overexpress both α and β isoforms of NRG-1 and, to a lesser extent, NRG-2. NRG-1β is a potent mitogen for nonneoplastic human (15, 34), monkey (35), and rat (16, 36) Schwann cells, suggesting that these NRG isoforms promote inappropriate proliferation of neoplastic Schwann cells in schwannomas. In contrast, NRG-1α does not promote Schwann cell proliferation (36). However, this does not mean that NRG-1 α proteins have no effects on neoplastic Schwann cells. In microarray experiments comparing the effects NRG-1α and NRG-1β have on the transcriptome of nonneoplastic Schwann cells, we have confirmed that NRG-1α stimulation triggers a number of transcriptional alterations in these glia (S. L. Carroll and M. S. Stonecypher, unpublished observations). The effects NRG-2 α and β have on Schwann cell mitogenesis have not yet been studied in detail, but NRG-2 α and β isoforms similarly differ in their ability to stimulate the proliferation of breast cancer cell lines (29). Considered together with previous work indicating that NRG-1 and NRG-2 elicit distinct biologic responses in at least some cell types (37), these observations suggest that NRG-1α, NRG-1β, NRG-2α, and NRG-2β will have isoform-specific effects on neoplastic Schwann cells.

The expression of multiple transmembrane precursors from the class II and class III NRG-1 subfamilies likely further diversifies NRG-1 signaling in human schwannomas. Class II (GGF) NRG-1 proteins are heparin-binding molecules that are released from the cells synthesizing them. After release, GGF proteins act as paracrine or autocrine signaling molecules that accumulate at high concentrations in structures such as the basement membranes that individually invest neoplastic Schwann

cells within schwannomas. In contrast, class III NRG-1 proteins remain membrane-associated and likely function only as juxtacrine signaling molecules (21). Our data thus supports a model in which NRG-1 promotes schwannoma formation in a complex process involving paracrine, autocrine, and/or juxtacrine signaling.

Before this study, there have been conflicting reports as to whether NRG receptors are expressed in human schwannomas. Hansen and Linthicum found that vestibular schwannomas demonstrated immunoreactivity for erbB2, erbB3, and NRG-1 (38). However, 2 other groups recently reported that erbB2 (39, 40) and erbB3 (40) expression is absent or only very weakly detectable in schwannomas. Using immunoblot, RT-PCR, real-time quantitative PCR, and immunohistochemical analyses, we found that erbB2 and erbB3 were readily detectable in schwannomas. ErbB2 and erbB3 were also the most commonly expressed erbB kinases in schwannomas, with protein and mRNA for these receptors uniformly expressed in our first series of tumors (Table 1) and 4 of 6 neoplasms demonstrating immunoreactivity for both kinases in our second series (Table 2). To further confirm the immunohistochemical findings described in this article, we subsequently immunostained a third series of 29 eighth cranial nerve schwannomas (27 sporadic, 2 NF2-associated) using different erbB2 and erbB3 antibodies (data not shown); immunoreactivity for both erbB2 and erbB3 was present in 27 of these tumors, including both NF2-associated schwannomas. We conclude that erbB2 and erbB3 are indeed expressed by neoplastic Schwann cells within nearly all schwannomas and that these tumor cells are potentially responsive to NRG-1 and NRG-2 produced endogenously in schwannomas.

In contrast to relatively slowly growing and benign schwannomas, neurofibromas can become quite large and transform into aggressive sarcomas (i.e. MPNSTs). We have recently demonstrated that autocrine and/or paracrine NRG-1/erbB signaling promotes neoplastic Schwann cell proliferation in human neurofibromas and MPNSTs (41) and that transgenic mice expressing the NRG-1 isoform GGFβ3 in myelinating Schwann cells develop neoplasms with morphologic, immunohistochemical, and ultrastructural features highly similar to those of human MPNSTs (42). Because our earlier work and the findings described here indicate that inappropriate NRG/erbB signaling may be an important factor in the pathogenesis of neurofibromas, MPNSTs, and schwannomas, it must be asked why inappropriate NRG-1/erbB signaling in these 3 different types of peripheral nerve sheath tumors is associated with such major differences in clinical behavior. In part, this is likely explained by differences in the genetic abnormalities that accompany NRG/erbB signaling in each tumor type. As noted, schwannomas typically develop mutations in the *NF2* tumor-suppressor gene. In contrast, neurofibromas demonstrate loss of neurofibromin expression and, as they progress and become MPNSTs, abnormalities in additional tumor-suppressor genes, including *p53*, *INK4A*, and $p27^{kip1}$ (43). Another possibility is that schwannomas, neurofibromas, and MPNSTs are derived from cells corresponding to different stages of differentiation in the Schwann cell lineage and that NRG/erbB signaling has distinct effects in these different contexts. This hypothesis is consistent with the observation that schwannomas typically show features highly similar to mature Schwann cells, whereas MPNSTs demonstrate a capacity for divergent differentiation reminiscent of multipotent neural crest stem cells (43). Finally, it is evident that schwannomas and neurofibromas/MPNSTs have significant differences in their pattern of NRG and erbB expression. Of particular note, we have detected NRG-2 expression in schwannomas (this work), whereas we did not find evidence for NRG-2 expression in neurofibromas or MPNSTs (41). In addition, although we only occasionally found evidence of increased EGFR expression in schwannomas, many neurofibromas and MPNSTs express elevated levels of this receptor (32, 41).

Of the other 8 NRG and EGF ligands, only HB-EGF, epiregulin, and TGFα were expressed in the majority of the schwannomas we examined. In contrast, relatively high-level expression of erbB4, which is activated by HB-EGF and epiregulin, was evident only in a subset of these neoplasms, whereas detectable expression of EGFR protein, which is the receptor for all 3 of these ligands, was evident in only one tumor. Nonetheless, we cannot exclude the possibility that HB-EGF, epiregulin, or TGFα also contributes to the pathogenesis of at least a subset of schwannomas expressing erbB4 and EGFR. Both erbB4 and EGFR are capable of heterodimerizing with erbB2 and erbB3 (44), indicating that ligands activating erbB4 and EGFR can "crosstalk" with erbB2 and erbB3 and thus modify cellular responses triggered by NRG-1 or NRG-2 stimulation. In addition, NRG-1 and NRG-2 can also act through erbB4; because each of the 4 erbB kinases activate distinct profiles of cytoplasmic-signaling effectors (44), NRG actions in erbB4-expressing schwannomas may differ from those evident in tumors lacking this kinase.

In summary, our findings support the hypothesis that autocrine, paracrine, and/or juxtacrine signaling by multiple NRG-1 and NRG-2 isoforms promotes the pathogenesis of human schwannomas. Because erbB neutralizing antibodies such as Herceptin and small molecular erbB inhibitors are effective in treating other tumor types, these observations suggest that inhibiting the NRG/erbB signaling may be an effective means of treating patients with surgically unresectable schwannomas. Establishing the role individual erbB kinases and specific NRG-1 and NRG-2 isoforms play in schwannoma tumorigenesis will be important for the development of innovative new approaches to treating these peripheral nerve sheath tumors.

## ACKNOWLEDGMENTS

*The authors thank Dr. Kevin A. Roth (Department of Pathology, UAB) for helpful comments on the manuscript.*

## REFERENCES

1. Woodruff JM, Kourea HP, Louis DN, et al. Schwannoma. In: Kleihues P, Cavenee WK, eds. Pathology and Genetics of Tumors of the Nervous System, 1st ed. Lyon: IARC Press; 2000:164–66
2. Reed N, Gutmann DH. Tumorigenesis in neurofibromatosis: New insights and potential therapies. Trends Mol Med 2001;7:157–62
3. Xiao G-H, Chernoff J, Testa JR. *NF2*: The wizardry of merlin. Genes Chromosomes Cancer 2003;38:389–99

4. MacCollin M, Woodfin W, Kronn D, et al. Schwannomatosis: A clinical and pathologic study. Neurology 1996;46:1072–79
5. Rowe JG, Radatz MW, Walton L, et al. Gamma knife stereotactic radiosurgery for unilateral acoustic neuromas. J Neurol Neurosurg Psychiatry 2003;74:1536–42
6. Gusella JF, Ramesh V, MacCollin M, et al. Merlin: The neurofibromatosis 2 tumor suppressor. Biochim Biophys Acta 1999;1423:M29–36
7. Gutmann DH. The neurofibromatoses: When less is more. Hum Mol Genet 2001;10:747–55
8. Sainz J, Huynh DP, Figueroa K, et al. Mutations of the neurofibromatosis type 2 gene and lack of the gene product in vestibular schwannomas. Hum Mol Genet 1994;3:885–91
9. Huynh DP, Maunter V, Baser ME, et al. Immunohistochemical detection of schwannomin and neurofibromin in vestibular schwannomas, ependymomas and meningiomas. J Neuropath Exp Neurol 1997;56:382–90
10. Hitotsumatsu T, Iwaki T, Kitamati T et al. Expression of neurofibromatosis 2 protein in human brain tumors: An immunohistochemical study. Acta Neuropathol 1997;93:225–32
11. Leone PE, Bello MJ, Mendiola M, et al. Allelic status of 1p, 14q, and 22q and NF2 gene mutations in sporadic schwannomas. Int J Mol Med 1998;1:889–92
12. Warren C, James LA, Ramsden RT, et al. Identification of recurrent regions of chromosome loss and gain in vestibular schwannomas using comparative genomic hybridisation. J Med Genet 2003;40:802–806
13. Brockes JP, Breakefield XO, Martuza RL. Glial growth factor-like activity in Schwann cell tumors. Ann Neurol 1986;20:317–22
14. Dong Z, Brennan A, Liu N, et al. Neu differentiation factor is a neuron–glia signal and regulates survival, proliferation and maturation of rat Schwann cell precursors. Neuron 1995;15:585–96
15. Morrissey TK, Levi ADO, Nuijens A, et al. Axon-induced mitogenesis of human Schwann cells involves heregulin and p185erbB2. Proc Natl Acad Sci U S A 1995;92:1431–35
16. Rahmatullah M, Schroering A, Rothblum K, et al. Synergistic regulation of Schwann cell proliferation by heregulin and forskolin. Mol Cell Biol 1998;18:6245–52
17. Carroll SL, Miller ML, Frohnert PW, et al. Expression of neuregulins and their putative receptors, ErbB2 and ErbB3, is induced during Wallerian degeneration. J Neurosci 1997;17:1642–59
18. Gerecke KM, Wyss JM, Karavanova I, et al. ErbB transmembrane tyrosine kinase receptors are differentially expressed throughout the adult rat central nervous system. J Comp Neurol 2001;433:86–100
19. Peles E, Yarden Y. Neu and its ligands: From an oncogene to neural factors. Bioessays 1993;15:815–24
20. Wen D, Suggs SV, Karunagaran D, et al. Structural and functional aspects of the multiplicity of neu differentiation factors. Mol Cell Biol 1994;14: 1909–19
21. Falls DL. Neuregulins: Functions, forms, and signaling strategies. Exp Cell Res 2003;284:14–30
22. Fischbach GD, Rosen KM. ARIA: A neuromuscular junction neuregulin. Annu Rev Neurosci 1997; 20:429–58
23. Ben-Baruch N, Yarden Y. Neu differentiation factors: A family of alternatively spliced neuronal and mesenchymal factors. Proc Soc Exp Biol Med 1994;206:221–27
24. Sandrock AW Jr, Goodearl ADJ, Yin Q-W, et al. ARIA is concentrated in nerve terminals at neuromuscular junctions and at other synapses. J Neurosci 1995;15:6124–36
25. Carraway KL, Weber JL, Unger MJ, et al. Neuregulin-2, a new ligand of ErbB3/ErbB4-receptor tyrosine kinases. Nature 1997;387:512–16
26. Chang H, Riese DJ, Gilbert W, et al. Ligands for ErbB-family receptors encoded by a neuregulin-like gene. Nature 1997;387:509–12
27. Busfield SJ, Michnick DA, Chickering TW, et al. Characterization of a neuregulin-related gene, Don-1, that is highly expressed in restricted regions of the cerebellum and hippocampus. Mol Cell Biol 1997;17: 4007–14
28. Higashiyama S, Horikawa M, Yamada K, et al. A novel brain-derived member of the epidermal growth factor family that interacts with erbB3 and erbB4. J Biochem 1997;122:675–80
29. Nakano N, Higashiyama S, Kajihara K, et al. NTAKα and β isoforms stimulate breast tumor cell growth by means of different receptor combinations. J Biochem 2000;127:925–30
30. Citri A, Skaria KB, Yarden Y. The deaf and the dumb: The biology of erbB-2 and erbB-3. Exp Cell Res 2003;284:54–65
31. Carpenter G. ErbB-4: Mechanism of action and biology. Exp Cell Res 2003;284:66–77
32. DeClue JE, Heffelfinger S, Benvenuto G, et al. Epidermal growth factor receptor expression in neurofibromatosis type 1-related tumors and NF1 animal models. J Clin Invest 2000;105:1233–41
33. Perry A, Kunz SN, Fuller CE, et al. Differential *NF1*, *p16*, and *EGFR* patterns by interphase cytogenetics (FISH) in malignant peripheral nerve sheath tumor (MPNST) and morphologically similar spindle cell neoplasms. J Neuropath Exp Neurol 2002;61:702–709
34. Levi ADO, Bunge RP, Lofgren JA, et al. The influence of heregulins on human Schwann cell proliferation. J Neurosci 1995;15:1329–40
35. Adalid-Avellana V, Bachelin C, Lachapelle F, et al. *In vitro* and *in vivo* behaviour of NDF-expanded monkey Schwann cells. Eur J Neurosci 1998;10:291–300
36. Raabe TD, Clive DR, Neuberger TJ, et al. Cultured neonatal Schwann cells contain and secrete neuregulins. J Neurosci Res 1996;46: 263–70
37. Crovello CS, Lai C, Cantley LC, et al. Differential signaling by the epidermal growth factor-like growth factors neuregulin-1 and neuregulin-2. J Biol Chem 1998;273:26954–61
38. Hansen MR, Linthicum FH Jr. Expression of neuregulin and activation of erbB receptors in vestibular schwannomas: Possible autocrine loop stimulation. Otol Neurotol 2004;25:155–59
39. Schlegel J, Muenkel K, Trenkle T, et al. Expression of the ERBB2/neu and neurofibromatosis type 1 gene products in reactive and neoplastic Schwann cell proliferation. Int J Oncol 1998;13:1281–84
40. O'Reilly BF, Kishore A, Crowther JA, et al. Correlation of growth factor receptor expression with clinical growth in vestibular schwannomas. Otol Neurotol 2004;25:791–96
41. Stonecypher MS, Byer SJ, Carroll SL. Activation of the neuregulin-1/erbB signaling pathway promotes the proliferation of neoplastic Schwann cells in human malignant peripheral nerve sheath tumors. Oncogene 2005; 24:5589–605
42. Huijbregts RPH, Roth KA, Schmidt RE, et al. Hypertrophic neuropathies and malignant peripheral nerve sheath tumors in transgenic mice overexpressing glial growth factor β3 in myelinating Schwann cells. J Neurosci 2003;23:7269–80
43. Carroll SL, Stonecypher MS. Tumor suppressor mutations and growth factor signaling in the pathogenesis of NF1-associated peripheral nerve sheath tumors. I. The role of tumor suppressor mutations. J Neuropath Exp Neurol 2004;63:1115–23
44. Yarden Y, Sliwkowski M. Untangling the erbB signaling network. Nat Rev Mol Cell Biol 2001;2:127–37


 